Quantification of Heavy Metals in Shoreline Sand of the Brahmaputra River via ICP-MS: A Case Study from Jorhat, Assam

A dissertation submitted for the partial fulfilment of the requirements for the degree of B. Sc. in Chemistry (Paper DSE-603) under Dibrugarh University

Under the Supervision of

Dr. Binoy K. Saikia

Principal Scientist

Coal and Energy Group, CE & MSD

CSIR-NEIST, Jorhat, Assam

Submitted By

Bikyparna Gogoi

Roll No: 14720008

Registration No: S2205341

Department of Chemistry

B.Sc. 6th Semester

N.N. Saikia College, Titabor-785630

Year: 2025

Dr. Jayanta Madhab Borah
Assistant Professor & HOD
Email: jayantamb@gmail.com

Department of Chemistry
Nanda Nath Saikia College
Titabar-785630, Assam, India

CERTIFICATE

*This is to certify that the dissertation entitled "**Quantification of Heavy Metals in Shoreline Sand of the Brahmaputra River via ICP-MS: A Case Study from Jorhat, Assam**" is submitted by **Bikyparna Gogoi**, a B.Sc. 6th semester student of the Department of Chemistry, N. N. Saikia College, Titabar for the partial fulfillment of B.Sc. degree in Chemistry (Paper: DSE-603), is a record of original research work carried out by him under the supervision of **Dr. Binoy K. Saikia**, Principal Scientist, CSIR-NEIST, Jorhat. He has fulfilled all the requirements for submitting the dissertation for the B.Sc. degree. The results embodied with this dissertation have not been submitted to any other college or institute for any other degree or diploma to the best of my knowledge.*

29/05/25

Date: 29/05/2025
Place: Titabar

(Jayanta Madhab Borah)

29/05/2025
....
(Internal Examiner)

29/05/25
....
(External Examiner)

CERTIFICATE

CONNECTING SCIENCE & TECHNOLOGY
NEIST
FOR A BRIGHTER TOMORROW

This is to certify that the project report entitled ***"Quantification of Heavy Metals in Shoreline Sand of the Brahmaputra River via ICP-MS: A Case Study from Jorhat, Assam"***, submitted by ***Bikyparna Gogo**i*, student of B.Sc. 6th semester, Department of Chemistry, Nanda Nath Saikia College, Titabor, Jorhat, Assam embodies the winter training carried out by him under my supervision during the period from 01/12/2024 to 20/01/2025 at Coal & Energy Group, CEMSD, CSIR-North East Institute of Science and Technology Jorhat, Assam.

He has completed his internship work at our respective division. I wish him all success in life.

Date: 06/05/2025

(Dr. Binoy K Saikia)
Principal Scientist,
Head, Coal & Energy Group,
CEMSD
CSIR-NEIST, Jorhat, Assam.

DECLARATION BY CANDIDATE

I hereby declare that the project report titled ***"Quantification of Heavy Metals in Shoreline Sand of the Brahmaputra River via ICP-MS: A Case Study from Jorhat, Assam"*** submitted to the Department of Chemistry, Nanda Nath Saikia College, Titabor in partial fulfilment of the requirement of the award of the Bachelor Degree of Science in a record of Bonafide work carried out under the supervision of ***Dr. Binoy K Saikia***, Principal Scientist, CSIR-NEIST, Jorhat. The matter embodied in this project has not been submitted by us for the award of any other degree.

Date: 06/05/2025

Place: Titabor, Jorhat, Assam

Bikyparna Gogoi

Bikyparna Gogoi

ACKNOWLEDGEMENT

I want to express my heartfelt appreciation to **Dr. Binoy Kumar Saikia**, Principal Scientist at the Coal and Energy Division of CSIR-NEIST in Jorhat, for introducing this topic and for his motivating guidance, constructive feedback, and invaluable suggestions throughout this project. His extensive knowledge and expert oversight, along with his unwavering patience, greatly supported my work at every phase. It is important to note that without his kindness and encouragement, completing this task would have been quite challenging.

I am truly thankful **to Dr. Virendra M. Tiwari**, Director of CSIR-NEIST in Jorhat, for granting me the opportunity to work at this prestigious institute.

I sincerely thank **Mr. Binud Attry** and all the senior research scholars of the Coal and Energy Group for their valuable help and guidance throughout my project.

I am extremely appreciative of my Principal **Dr. Litool Baruah** and **Dr. Jayanta Madhab Bora**, Head of the Department of Chemistry at Nanda Nath Saikia College, Titabor for allowing me to undertake my work at CSIR-NEIST, which made it possible for me to gain such valuable analytical skills.

I would also like to offer my sincere thanks to all my colleagues (Sonkalpita Baruah, Priya Saikia, Ankur Borah, Priyanuj Hazarika, Justin Sanga, Pinky Chutia, Gongutri Saikia and Hemanta Phukan) and especially all the staff members of the Coal and Energy Group at CSIR-NEIST in Jorhat, for their support at various times.

Last but certainly not least, I extend my heartfelt thanks to all my friends and family members who have generously offered their assistance in completing this project.

Bikyparna Gogoi
Bikyparna Gogoi

TABLE OF CONTENTS

List of Figures

List of Tables

ABSTRACT

The current research examines the distribution and heavy metal concentration in Brahmaputra River shoreline sands around Jorhat, Assam. Sand samples were taken from three key positions—Shanti Ashram (SSA), 8 No Spur (S8NO), and Baghmora (SBM)—and subjected to Inductively Coupled Plasma Mass Spectrometry (ICP-MS) analysis after following routine sample preparation procedures such as air-drying, crushing, sieving, and microwave-assisted acid digestion. The findings showed substantial spatial variation in heavy metal composition, largely controlled by source rock lithology, weathering intensity, and sediment transport dynamics. Elevated levels of iron (Fe), chromium (Cr), and zinc (Zn) were recorded, with the highest Fe concentration at 8 No Spur (62,471.58 ppm) and the highest Zn at SSA-4 (50,543.4 ppm). Additional high Fe and Zn values were noted at SSA-2 and SBM-1/SBM-6. These findings highlight the geochemical diversity of the Brahmaputra River system and underscore the necessity for ongoing monitoring to assess the interplay of natural geologic processes.

Keywords: Heavy metals, Brahmaputra River, Shoreline sand, ICP-MS analysis, Geochemical characterization.

1.Introduction:

Sand is a naturally occurring granular material composed predominantly of finely divided mineral particles and rock fragments, generally between 0.0625 and 2 millimeters in diameter. These minute particles are almost entirely constituted by silicon dioxide (SiO_2), commonly known as silica, mainly in the form of quartz, although the mineralogical composition may vary much depending on local conditions of geology and formation. They can include other minerals in smaller proportions, usually feldspar, mica, and various heavy minerals. Sand originates from the continued weathering and erosion of larger rock formations, where mechanical and chemical processes break them down to their granular state. These particles may be transported and deposited by different geological agents such as wind, water, and glacial activity, and have differing characteristics related to grain size, shape, and sorting. It is these physical properties of sand, including grain size distribution, sphericity, and angularity, that determine how sand behaves in nature and in most engineering applications. The chemical makeup of sand, dominated by its high silica content, is mostly made up of the mineral quartz (SiO_2), which usually constitutes about 70% to 90% of most samples of sand and depends on its geological source. Apart from the silica, the minerals of the feldspar group, which generally include both the orthoclase and plagioclase types, may account for about 5% to 15% of the whole mass. Mica, another quite common constituent, usually makes up about 1% to 5%. Heavy minerals, zircon, rutile, and magnetite, usually amount to trace quantities, generally less than 1% to 5%. On the other hand, in marine and coastal settings, calcium carbonate ($CaCO_3$), a product of biogenic origin, may make up 1% to 10% of the matrix of sand; this would evidence the presence of fragments of shells and other calcareous materials within it. Iron oxides, which probably impart their distinctive colors to the sand, are generally present in minor concentrations usually less than 5%. In general, the complex chemical composition of sands would mirror the prevailing geologic processes and environmental conditions governing their formation, causing diversity among the types of sand in the same variety of geomorphological settings.

1.1 Classification of Sand:

According to United State Geological Survey (USGS) sand is classified as Fine Sand (0.075 to 0.425mm), Medium Sand (0.425 to 2mm), and Coarse Sand (2.0 mm to 4.75mm). Fine sand is the sand that passes through 16 number sieves (Test sieve with 1.18 mm openings and 304.8 mm or 152.4 mm diameter) and is most commonly used in plastering works. Medium sand (Moderately Coarse Sand) is the sand that passes through 8 number sieves (Test sieve with 2.3 mm openings and 203 mm diameter). It is used for mortar and masonry works. Coarse sand is the sand that passes through 4 number sieves (Aperture size of 4.75 mm) and is commonly used for concrete works [1].

Based on origin, sand is classified as Pit sand, River sand, Sea sand and Manufactured sand. Pit sand is commonly found in red-orange color and it is secured from deep pits dug 1 to 2 meters from below the topsoil. The grains of pit sands are rough, angular, sharp and harsh. It is free from salts and other impurities because of which it is a conventional selection for concreting. The grains of pit sands are rough, angular, sharp and harsh. Sea sand refers to the sand eroded by seawater and it is secured from seashores and has a distinct brown color. The grains of sea sands are very fine in quality with a circular shape. Sea sand consists of salt and other marine impurities which tend to absorb atmospheric moistness and bring forth dampness. Manufactured sand (M-sand) created by crushing hard granite stones, manufactured sand refers to an artificially created type of sand made as an alternative to river sand for construction [2]. Utility sand is a coarse natural sand that is commonly applied to backfill, fill trenches, and as a base course for pavers or slabs, providing good compaction and economy. Concrete sand, on the other hand, is a washed, coarse sand specially graded and cleaned for concrete production, providing strong bonding, proper drainage, and maximum strength in construction uses.

Fig 1: Pictures of different types of sands.

1.2 Chemical Composition of Sand:

The granular materials are unconsolidated, consisting of either lithic fragments or mineral particulates, which often come from terrestrial or marine sources. Silicate minerals make up the bulk of sand, with quartz being the most abundant because of its high resistance to weathering processes. This is because quartz has a very robust crystalline structure that can withstand mechanical and chemical degradation over time. Other than quartz, the major rock-forming minerals such as amphiboles and micas can also be present in the matrices of sand. These minerals are less abundant but add more diversity in the mineral composition of sand deposits. Heavy minerals, among others present in trace quantities, such as tourmaline, zircon, and rutile, can be present in sedimentary environments that result from selective transport and deposition. The heavy metal content of sand greatly depends on the source and conditions of the environment. Some common heavy metals detected in sand include arsenic (As), cadmium (Cd), chromium (Cr), copper (Cu), lead (Pb), nickel (Ni), and zinc (Zn). Concentration levels of these heavy metals have been proven to depend on industrial activities, natural geological processes, and urban runoff.

Table 1: Chemical constituents of sand.

Chemical constituents	**Typical composition range (%)**	**Primary Minerals**
Silicon dioxide (SiO_2)	95.0 – 99.5	Quartz
Aluminum oxide (Al_2O_3)	0.1 – 2.5	Feldspar, micas
Iron oxide (Fe_2O_3)	0.01 – 1.0	Magnetite, hematite
Calcium oxide (CaO)	0.1 – 0.5	Calcite, dolomite
Magnesium oxide (MgO)	0.05 – 0.4	Dolomite, hornblende
Potassium oxide (K_2O)	0.1 – 0.8	Orthoclase, microcline
Sodium oxide (Na_2O)	0.05 – 0.5	Albite, plagioclase
Titanium dioxide (TiO_2)	0.01 – 0.2	Rutile, ilmenite
Trace elements	0.1	Various accessory minerals

Table 2: Elemental Composition of sand.

Element present	Percentage (%)
Alumina	13.86
Silica	79.98
Calcium	0.87
Titanium	0.15
Potassium & Sodium	1.89
Iron	1.89
Manganese	1.44

1.3 Geological Formation of River Sand:

The formation of river sand is a multi-step process involving weathering, erosion, sediment transport and deposition. Initially, weathering breaks down rocks into smaller particles, creating the sand-sized grains essential for river sand formation. Following this, erosion removes these particles from their source, allowing rivers to transport them downstream. The movement of these sediments is governed by natural forces, primarily water, which plays a crucial role in carrying the sand-sized particles to new locations. Eventually, deposition occurs when these particles settle in areas such as river deltas or beaches, marking the final stage in the formation of river sand. Understanding these processes is vital in the field of fluvial geomorphology, which examines how rivers shape landscapes and contribute to sediment dynamics. This integrated approach highlights the interconnectedness of geological processes in the creation of river sand.

Weathering: Weathering is the process of breaking down rocks into smaller particles, which is the first step in the formation of river sand. It involves the physical and chemical disintegration of rocks due to exposure to wind, water, and temperature fluctuations. Weathering sets the stage for the creation of sand-sized particles that can be transported by rivers. The degree of chemical weathering (measured using the chemical index of alteration) increased with decreasing particle size of the sediment, which is consistent with the mineralogy of the size-fractioned sediments [3].

Erosion: Erosion is the process of wearing away and removal of rock particles from their source, which is a crucial step in the formation of river sand. Rivers, glaciers, and wind can cause erosion, transporting the broken-down particles downstream. Erosion helps to create the sand-sized particles that make up river sand.

Sediment transport: Sediment transport refers to the movement of sediment particles, including sand, by natural forces like water and wind. Rivers play a key role in sediment transport, carrying sand-sized particles from their source to their deposition point. Understanding sediment transport is essential to grasping the formation of river sand. Sediment transport processes have recently gained importance in river engineering, torrent control and reservoir management due to an increasing discrepancy between a surplus of sediments in upstream and a deficit in downstream river sections [4].

Deposition: Deposition is the process of sediment particles, including sand, coming to rest in a new location, such as a river delta or beach. Deposition is the final stage in the formation of river sand, where the sand-sized particles are deposited and accumulate. Deposition shapes the landscape and creates new landforms.

1.4 Heavy Metal Contamination and Properties of Indian River Sand:

River sand is created through the disintegration and deterioration of rocks into smaller fragments due to weathering and erosion processes, which could take thousands and millions of years. Its specific properties are its rounded and smooth grains, which are due to constant abrasion during its transportation process via rivers. In this way, it has proven easy to mix with and handle for concrete and mortar mixtures. River sand generally has a well-balanced particle size distribution or gradation, leading to improved packing density and reduced segregation in concrete mixes. Even with its lower angularity compared to crushed sand, its spherical shape can help to positively influence the strength and durability of concrete under certain pressures. The river sand, in many cases, is observed to have good cohesion and a bearing capacity when used for foundations and road constructions. Its relatively low porosity gives its low permeability, which in many applications is advantageous for drainage control. The properties of river sand in India have considerable effects on the behavior and mobility of heavy metals, playing a critical role in environmental health. Physical characteristics, such as the size, shape, and texture of the sand, determine which applications the sand will be suitable for and its ability to retain pollutants like heavy metals. Chemical composition in river sand also varies by geological location, affecting the types and concentrations of heavy metal contaminants present. Knowing the geochemical cycling of these metals through sedimentation and dissolution will help to determine their sources and sinks in the river systems. It is, therefore, necessary to develop remediation technologies aimed at removing or immobilizing heavy metals from contaminated river sand for mitigation of the associated environmental risks. The properties of Indian river sand, particularly from southern region like Ponnai River in Tamil Nadu, are characterized by a rich mineral composition and a relatively low concentration of heavy metals including Pb, Cr, Zn, Ni, Hg, As, Mn, and Cu, with Mn being the most abundant. In contrast, other Indian rivers like the Ganges show moderate to high ecological risks due to heavy metal contamination (Cr, Fe, Ni, Cu, Zn, Cd and Pb are present and Cd being a significant contaminant and agricultural activities contributing to toxicity), primarily from anthropogenic sources. Heavy metal concentrations in Narmada River sediments are increasing due to industrial development, posing environmental and health risks. Pollution indices indicate moderate contamination, with Cr, Mn, Cu and Pb being major contributors, while Mn and Cd pose high risk to aquatic organisms [5] [6] [7].

1.5 Distribution of Brahmaputra River Sand in Assam:

The distribution of Brahmaputra River sand across Assam is highly heterogeneous, influenced by the river's braided nature, local geomorphology and tectonic activity. In the upper reaches of Assam, the sand tends to be coarser and less mature, with a higher proportion of lithic fragments. As the river progresses through the Assam valley, the sand becomes finer and more compositionally mature. Extensive sand bars, mid-Channel Islands, and floodplain deposits characterize the river's course, with grain size generally decreasing downstream. However, local variations are significant, with coarser deposits often associated with tributary junctions and areas of channel constriction. The sand distribution is also influenced by the annual monsoon cycle, with high flows redistributing sediments and creating new depositional features. Anthropogenic activities, particularly sand mining and flood control measures, have locally altered natural sediment distribution patterns. The chemical and physical properties of the sand vary spatially, reflecting changes in source rock composition, weathering intensity, and transport distance. This variability in composition and distribution makes the Brahmaputra sand a complex but valuable resource, with implications for local ecology, geomorphology, and human use across the Assam region.

The Brahmaputra River sand exhibits a complex and varied chemical composition and distribution, reflecting the diverse geological terrain it traverses and the dynamic fluvial processes at work. Predominantly siliciclastic in nature, the sand is characterized by a high quartz content, typically ranging from 60-80%, with feldspars (both plagioclase and K-feldspars) forming the second most abundant mineral group at 10-25%. The remaining fraction consists of various accessory minerals including micas, amphiboles and heavy minerals such as garnet, zircon and rutile. The sand shows a high SiO_2 content (67.81-69.97%), moderate Al_2O_3 (12.12-13.45%), and lower concentrations of Fe_2O_3 (6.0-6.47%), CaO (3.36-3.74%) and minor amount of MgO, Na_2O, K_2O and other oxides reflecting the mature nature of the sediments and the weathering history of the source rocks. Trace elements and rare earth elements (REEs) are present in varying concentrations, providing valuable insights into sediment provenance and tectonic setting [8].

2. Objective of the Study:

a. To quantify the concentration of heavy metals in river sand samples using Inductively Coupled Plasma Mass Spectrometry (ICP-MS).

b. To analyze the geochemical composition and spatial distribution of heavy metals in river sediments through precise sample preparation and advanced analytical techniques.

2.1 Literature Review:

Chakarvorty et al. (2015) examined the influence of urban sewage on heavy metal pollution in the Ganga and Yamuna rivers in India, taking the city of Allahabad as a case study. Geochemical and magnetic susceptibility measurements were combined to explore 29 samples of water collected from sewage and river confluence sites in Allahabad. Their geochemical analysis revealed a significantly higher concentration of heavy metals, such as Pb, Zn, V, Ni, Cr, Co, and Mn, compared to the concentrations in the river water samples in sewage and mixed water samples, hence indicating heavy metal contamination primarily from anthropogenic sources. For the seven elements evaluated, Co, Mn, Pb, Ni, Cr, V, and Zn, the enrichment ratios calculated were quite high compared with the UCC, though the highest was for Zn and then V, Cr, Ni, Pb, Mn, and Co, in that order. The authors have also discussed how anthropogenic pollutants may influence the REE contents of the sediments. They found that although the overall REE patterns showed some degree of fractionation, the high concentrations of some elements and a positive Gd anomaly suggested a significant influence of anthropogenic sources. This study concluded that the elevated heavy metal and REE concentrations in the rivers are primarily due to the discharge of untreated sewage from urban areas and industrial activities [9].

Falciani et al. (2000) reviewed the method for the multi-element analysis of V, As, Co, Hg, Cd, Mo, Sn, Ba, Be, Cr, Ni, Pb, Cu and Zn in soils and sediments by means of inductively coupled plasma-mass spectrometry (ICP-MS) after microwave-assisted digestion. The overall method employed microwave digestion procedure via a mixture of HNO_3-HF towards complete sample dissolution. The authors stated that the signal suppression due to HNO_3 has been noticed for the elements which have a high ionization potential, such as Zn, As and Cd. Consequently, calibration solutions have to be prepared with exactly the same acids used for the mineralization of samples. Using this approach, they got very low values of the limit of quantification, most of them being less than 100 µg/ kg. The accuracy was better than 80% for most of the elements and good precision values were obtained, as relative standard deviation, in the range of 0.3–14% [10].

Suleman and ElAgib (2015) conducted a study to analyze the chemical composition of the collected sand samples from the Nafud Desert, Saudi Arabia, in Zilfi Province. 21 elements in 21 samples of sand were analyzed using Inductively Coupled Plasma-Mass Spectrometry (ICP-MS). The content of the study indicated that trace toxic elements, especially Ni, Cd, and As, were higher than background values for sandstone as compared with literature values. Their study further revealed that the highest concentrations of elements such as Pb, Zn, Na, Ca, and Cd were observed in the Al-Sabla region, which is close to a city and thus exposed to contamination. However, the highest concentrations of As and V were found in the Shlwan region, and the highest concentration of Cr was found in the Alaaga region. Concentration maximums, including Co, Ti, P, Fe, Al, and Mg, for elements were predominantly seen in the Magra area. The general observations deduced from the author's study indicated a high potential chemical content of Nafud sand to be further employed for industrial processes such as glass [11].

Veerasamy et al. (2021) presented an exhaustive study of the concentration of trace elements (TEs) and rare earth elements (REEs) in the beach placer deposits of Odisha, India, by inductively coupled plasma mass spectrometry (ICP-MS). The method was validated through certified reference materials with recovery ranges between 90% to 110%, implying high analytical precision. Their study indicated enrichments of some elements to levels significantly higher, such as Cr, Mn, Fe, Co, Zn and Th; the total content of REEs ranged from 101.3 to 12,911.3 µg/g, much higher than the average crustal values. The enrichment factor (EF) and geo-accumulation index (I_{geo}) analyses suggested that the observed enhancement in TEs and REE is primarily natural in origin because of the abundance of REE-bearing minerals such as monazite rather than due to anthropogenic influence. Correlation between Th and light REE also signifies the geological source of these elements from felsic rocks present in the hinterland, mainly granite and charnockite [12].

Aggarwal et al. (2024) reported a study on heavy metal concentrations in suspended sediments along the Ganges River reveals the urgent issue of anthropogenic pollution in aquatic ecosystems via Atomic Absorption Spectrometry (AAS) and ICP-MS. Interestingly, this study averaged different metals in the region: iron at 50,230 µg/g, manganese at 1,283 µg/g, chromium at 201 µg/g, zinc at 183 µg/g, lead at 55.1 µg/g, nickel at 50.9 µg/g, copper at 42.8 µg/g, and cadmium at 1.01 µg/g. This shows a very high concentration of contaminants in the area. The analysis used a range of pollution indicators. They found that there were moderate degrees of contamination for chromium across the area of study, with a GI (Geographical Indication) ranging between 0 and 1 at upstream locations while for locations below the enrichment zone there was an uncontaminated to moderate status. ER (Ecological Risk) values between 1 and 3 shows minor enrichment of chromium throughout the study area while the PLI (Pollution Load Index) values, that ranged between 0.72 and 0.86, indicated an overall uncontaminated status of the river segment [13].

3. Method and Methodologies:

3.1 Study Area:

The Brahmaputra River emanates from the Chemayungdung Glacier situated within the Tibetan Plateau, specifically in the southwestern region of Tibet, where it is designated as the Yarlung Tsang Po. Progressing in an easterly direction for approximately 1,625 kilometers, it undergoes a significant deviation at the Namcha Barwa peak prior to traversing into India via the Kepang La Pass in Arunachal Pradesh, where it is identified as the Siang or Dihang River. The Brahmaputra extends to an approximate length of 2,900 kilometers, thereby ranking it among the longest rivers globally; it is characterized by a broad, braided channel, particularly evident in Assam, where its width may expand to as much as 10 kilometers during the monsoon season. The river has a high discharge rate, estimated to be around 19,800 cubic meters per second and carries a huge sediment load that is crucial for the fertility of the floodplain alongside. The Brahmaputra River passes through the Jorhat district of Assam marking its northern boundary. This celebrated river has a longitude of approximately 94.2° E and an elevation of about 100 meters above sea level. It plays an important role in the local environment and supports the means of livelihood for the people dwelling along its shores. The river is characterized by its long, braided courses, especially during the monsoon season when it is swollen up to a width of more than 5 miles (8 km) at times. The Brahmaputra is not just vital for irrigation and agricultural projects but also plays the role of a main transport route for transporting commodities and human resources in the region. Banks are covered with greenery and river supports numerous types of vegetation and fauna; thus, rich biodiversity characteristic to Assam increases further. Picnic spots in Jorhat district along the Brahmaputra River have distinctive patterns of sand distribution that add to their natural beauty and recreational value. Along the banks and bars, the river deposits fine to medium-grained sand that makes for vast, sandy beaches for picnics and recreation. The sand typically grades gently from coarse near the edge of the water to finer landward. The sand distribution varies seasonally, as monsoon floods reshape the sandbanks and beaches annually. During the dry season, the exposed sandbars are natural recreational spaces with clean, light-colored sand that is comfortable for visitors to sit and walk on. Kokilamukh Picnic Spot (about 12.3 km from the town of Jorhat and situated close to Shanti Ashram with coordinates of Latitude: 26°49'39"N and Longitude: 94°05'10"E), 8 No Spur (about 16.8 km from Jorhat town and coordinates of Latitude: 26°50'12.26"N and Longitude: 94°14'24.81"E), and Baghmora (16.5 km away from the town of Jorhat with coordinates of Latitude: 27°11'25.1"N and Longitude: 94°40'12.8"E) are visually pleasing picnic sites and stand along the sides of the magnificent Brahmaputra River, popular for their silky white beaches and lush greens. These areas have a patchy distribution of shoreline sands, which are shaped by the natural forces of the Brahmaputra, including sedimentation and erosion, which are highly variable in response to seasonal changes and fluctuations in water levels. During the dry season, when the water level recedes, more sandy land is exposed, thus creating ideal conditions for recreational picnicking. Whereas in the monsoon season, the sandy sites could be flooded.

3.2 Sample Collection:

The samples pertaining to the shoreline sand of the Brahmaputra River have been meticulously collected from three distinct locations, namely Shanti Ashram situated in Kokilamukh, 8 No Spur, and the picturesque Baghmora picnic spot, with an emphasis on extracting samples from a depth range extending from 1 foot to 6 feet beneath the surface of the shoreline at each of these specified locations during the winter season of 2024, thereby ensuring a comprehensive analysis of the sedimentary characteristics at varying depths. The aforementioned samples collected from Shanti Ashram, 8 No Spur, and Baghmora have been securely contained within plastic zip bags for preservation purposes and have been systematically labeled for identification in accordance with the following designations: SSA-1, SSA-2, SSA-3, SSA-4, SSA-5, SSA-6 for Shanti Ashram; S8 No-1, S8 No-2, S8 No-3, S8 No-4, S8 No-5, S8 No-6 for the S8 No Spur area; and SBM-1, SBM-2, SBM-3, SBM-4, SBM-5 and SBM-6 for the Baghmora location, thereby facilitating organized data management for subsequent analysis. The precise geographical coordinates of each sample location have been meticulously recorded utilizing a hand-held global positioning system (GPS) device, which measures the latitudinal and longitudinal positions in terms of degree-minute-second format, thus ensuring high accuracy in the spatial representation of the sampling sites. Each of the designated sampling locations is situated at an approximate distance of 5 kilometers from one another, and collectively, the study area encompasses a substantial distance of approximately 14 kilometers, thereby providing a significant spatial framework for the examination of shoreline sand characteristics along the Brahmaputra.

Table 3: Location data of sampling site with sample IDs.

Location	Sample ID	Depth	Latitude	Longitude
Shanti Ashram	SSA-1, SSA-2, SSA-3, SSA-4, SSA-5, SSA-6	1feet (surface) to 6 feet	26°49'39"N	94°05'10"E
8 No Spur	S8NO-1, S8NO-2, S8NO-3, S8NO-4, S8NO-5, S8NO-6	1feet (surface) to 6 feet	26°50'12.26"N	94°14'24.81"E
Baghmora	SBM-1, SBM-2, SBM-3, SBM-3, SBM-4, SBM-5, SBM-6	1feet (surface) to 6 feet	26°11'25.1"N	94°40'12.8"E

Fig 2: Location map of sampling areas (Shanti Ashram, 8 No Spur & Baghmora)

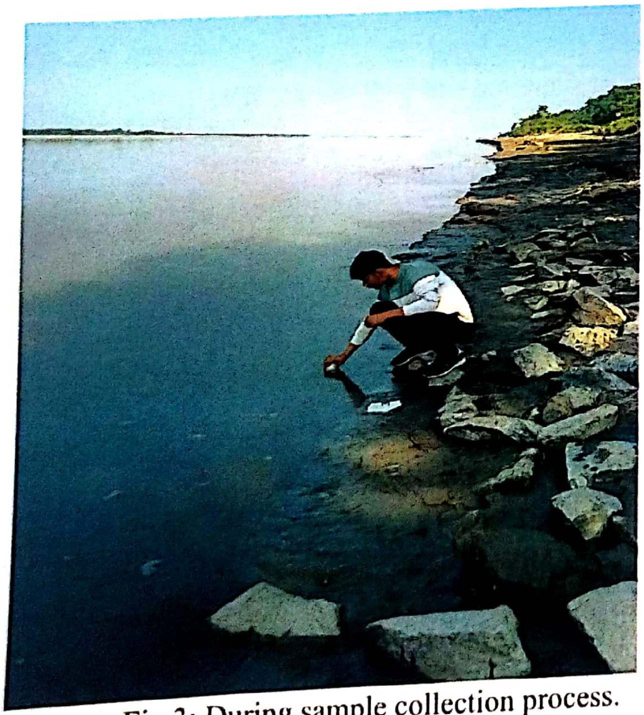

Fig 3: During sample collection process.

Fig 4: Collection of samples from different depths.

3.3 Sample Preparation:

Approximately 250 gm of 18 sand samples that had been meticulously collected were subjected to a process of air drying, utilizing the natural conditions of the open-air environment to facilitate this procedure. After the air-drying phase, the samples were then processed individually in the Rotor Beater Mill, where they undergo a crushing procedure at a rotational speed of 4000 revolutions per minute (rpm), ensuring thorough pulverization. Subsequently, the crushed samples were placed into the Sieve Shaker machine, calibrated to 72 British Standard (BS) sieves (212 µm) where they were subjected to vigorous shaking while ensuring that the samples were adequately packed for optimal separation and analysis.

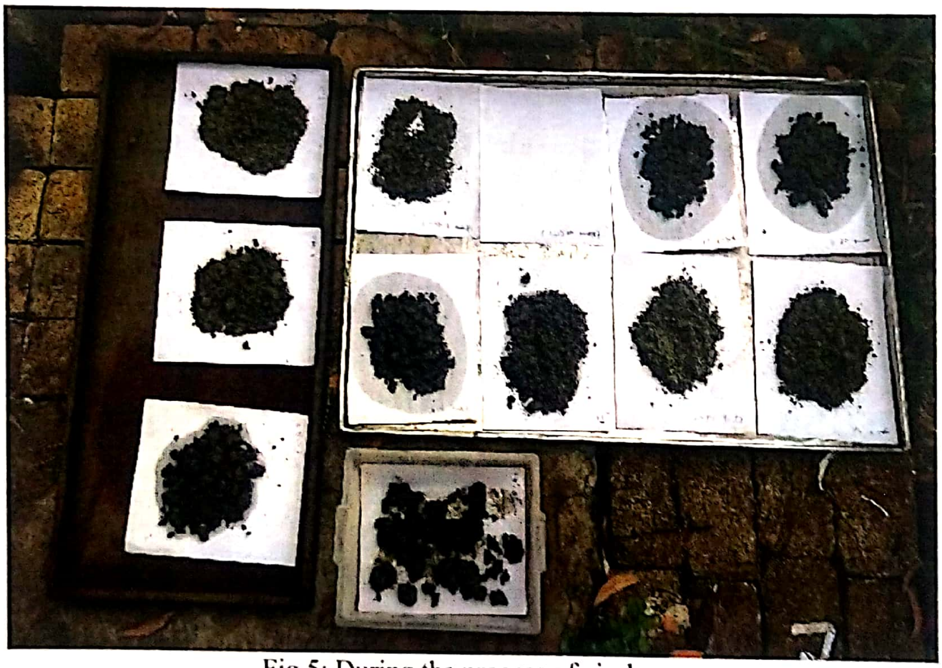

Fig 5: During the process of air dry

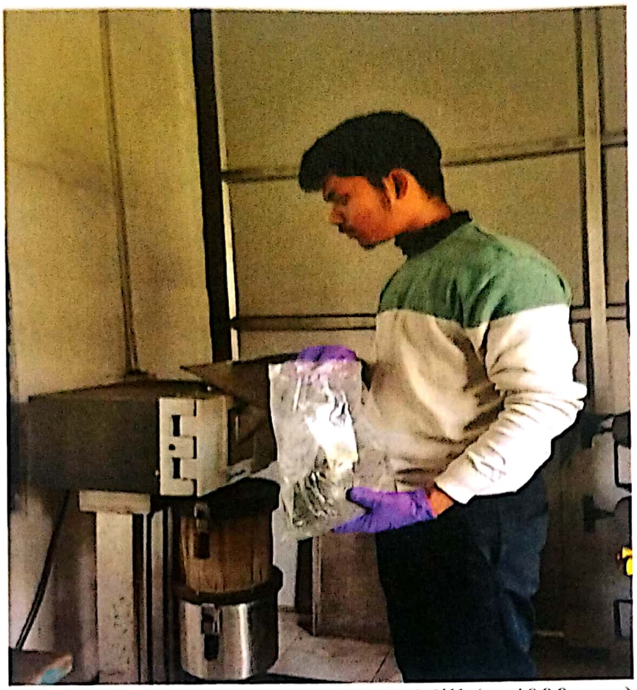

Fig 6: Grinding the sand samples in Rotor Beater Mill (at 4000 rpm) after air-dry.

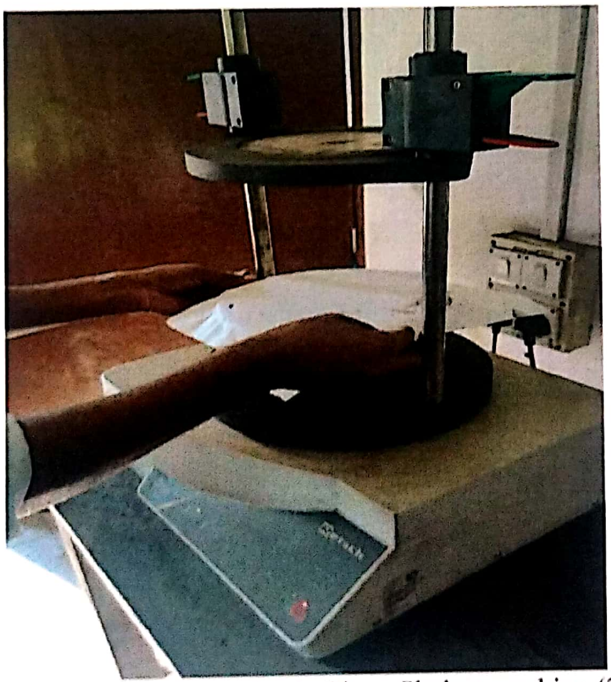

Fig 7: Crushing the sand samples in Sieve Shaker machine (212 μm)

3.4 Microwave-Assisted Digestion:

Weighing out 100 milligrams of sand from each prepared sample for the digesting process and packing it with aluminum foil. The microwave digestion vessels were filled with a solution of 2 ml concentrated nitric acid (HNO_3), 6 ml hydrogen fluoride (HF), and 2 ml hydrochloric acid (HCl) and add the weighed samples (100 mg. of sample + 2 ml of conc. HNO_3 + 6 ml of HF + 2 ml of conc. HCl). The vessels were then sealed and inserted into the microwave digesting system for 50 minutes. The digestion program was configured to progressively increase the temperature to a maximum of 200-300 °C while managing the pressure, which can reach up to 200 bar. After digestion was complete, the vessels were allowed to cool to room temperature and the digested samples were carefully transferred to centrifuge tubes (50 ml).

Fig 8: Microwave digestion vessels.

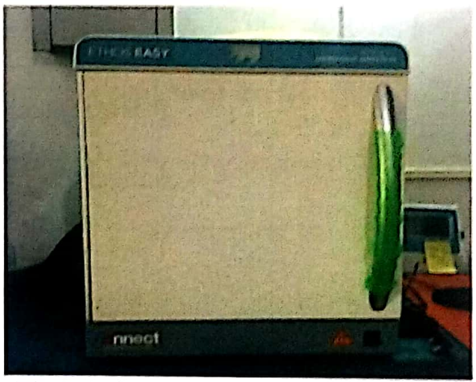

Fig 9: Microwave digesting system.

Fig 10: During the process of microwave digestion.

3.5 Sample Dilution:

In the specific sample dilution process, an exact volume of 2 ml of the previously digested sample solutions was meticulously combined with 38 ml of distilled water in 50 ml Griffin beakers. Approximately 13 ml of each of the 18 sample solutions was filtered using a syringe filter with a pore size of 0.22 microns, conducted in 15 ml centrifuge tubes, with all sample IDs clearly labeled.

3.6 Instrumentation:

The analytical determination of V, Mn, Fe, Cu, As, Au, Pb, Cr, Co, Cd and Zn was carried out by ICP-MS (Inductively Coupled Plasma-Mass Spectrometry). The table illustrates the operating conditions of the equipment utilized in this investigation.

Table 4: Conditions for ICP-MS.

RF power	1550 W
Plasma mode	Low matrix
Nebulizer gas flow	1.06 L/min
Lens voltage	9.0 V
Anglo stage voltage	2154 V
Scan mode	Peak hopping
Sample depth	8.0 mm

Reagents:

The following high purity acids are used:

Nitric Acid (HNO_3, ≥69% ultra-pure grade): Used as an oxidizing agent to dissolve metals and stabilize elements in solution.

Hydrochloric Acid (HCl, ≥ 37% ultra-pure grade): Helps in the dissolution of elements such as Pb. Ag, and Hg while preventing precipitation.

ICP-MS relies on ultra-high-purity gases to sustain plasma conditions and aid in ion transport.

The following gases are used:

Argon (Ar, 99.999% purity): Used as the plasma gas, auxiliary gas, and nebulizer gas.

Oxygen (O_2, 99.999% purity): Occasionally introduced to prevent carbon deposition when analyzing organic-rich sands.

3.7 Working Principle of ICP-MS:

The operation of Inductively Coupled Plasma Mass Spectrometry (ICP-MS) is based upon key principles that account for its extreme sensitivity and accuracy. At the heart of this process is inductive coupling, which utilizes a high frequency electromagnetic field to create a plasma, thus enabling the efficient ionization of sample atoms. The quality of plasma generated is important, since it directly influences the efficiency of ionization, allowing trace elements of key interest to be detected with remarkable precision. The separation and detection of these ions by mass spectrometry techniques are based on their mass-to-charge ratio after ionization, increasing the resolution and accuracy of the analysis. Furthermore, the quadrupole mass filter is involved in this separation process, where only ions of interest are detected, thus increasing the sensitivity of the measurements. The following principles together have enabled ICP-MS to analyze the extremely low concentration range of almost any element in samples.


Fig 11: ICP-MS working station in CSIR-NEIST.

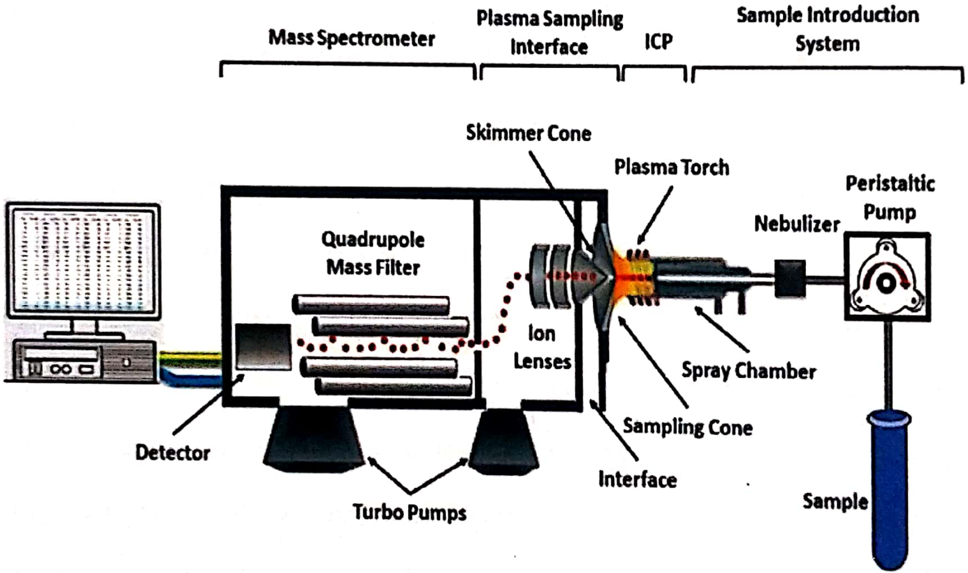

Fig 12: Schematic diagram of ICP-MS.

Inductive Coupling: ICP-MS uses a high frequency electromagnetic field to produce a plasma which helps in ionizing sample atoms. This allows efficient energy transfer from the electromagnetic field to the sample, giving ICP-MS the high sensitivity and accuracy that is inherent in the technology. The primary reason ICP-MS is essential is due to the induction of sample atom ionization. An annular slotted shield protects the inductive coupling element from the plasma, which also removes capacitive coupling from the element to the plasma and unwanted sputtering of the element. These conditions therefore make for proper inductive coupling of RF power into the plasma [14].

Plasma generation: In ICP-MS, generation of plasma is the most essential step where plasma of high temperature is produced from the interaction between the electromagnetic field and the sample. The efficiency in ionization of the atoms within the sample helps detect trace elements, as discussed below. Sensitivity and accuracy of ICP-MS highly depend on the quality of plasma formed. The plasma generating apparatus includes a RF generator for providing a RF power, an antenna for generating an electromagnetic field upon receiving the RF power, a reaction chamber for exciting/ionizing a reaction gas via the electromagnetic field, and generating a plasma, and a plasma channel for absorbing the RF power, and allowing a current signal to be induced to the plasma [15].

Ionization efficiency: The ICP-MS depends largely on ionization efficiency since it is what gives the number of ions formed from the atoms of the sample. High energy in the plasma, which forms from ICP-MS, causes the effective ionization of the sample atoms, and therefore it gives a very high sensitivity and accuracy for the trace element detection.

Mass Spectrometry: Mass spectrometry is considered as the backbone component of ICP-MS that separates and detects the ions through their mass to charge ratio generated. This has the capability of identifying and calculating the elements contained in the sample. The resolution and accuracy about the mass ICP-MS is attributed due to the better mass spectrometry techniques employed.

Quadrupole mass filter: It is one of the critical parts of ICP-MS that separates and detects ions according to their mass-to-charge ratio. The quadrupole mass filter is crucial for achieving the high mass resolution and accuracy required in ICP-MS. This enables the detection of trace elements in complex samples. An ion source located at the entrance of a quadrupole mass filter focuses a beam of positive ions to a point inside the quadrupole where the fringing field has a very much reduced effect on defocusing [16].

Detector technology: Detector technology is an essential aspect of ICP-MS in that it uses detectors to monitor the ions separated by the mass spectrometer. Advanced detector technologies such as pulse counting and analog detection make ICP-MS highly sensitive and accurate.

Radio frequency (RF) power: RF power is used to create the plasma in ICP-MS. The power level and frequency of the RF affects efficiency in the ionization process, which is important for the sensitivity of ICP-MS. Optimization of RF power is crucial for maximum sensitivity and accuracy.

Gas flow dynamics: Gas flow dynamics play a significant role in ICP-MS, as it involves the influence of argon and helium on plasma generation and ionization efficiency. The gas flow dynamics play a very critical role in ensuring high sensitivity and accuracy in ICP-MS.

Sample introduction: Sample introduction is a very crucial step in ICP-MS. This is because a sample is introduced into the plasma torch. The sample introduction system needs to be optimized so that it will have efficient ionization and detection of the sample atoms. The sensitivity and accuracy of ICP-MS may be affected by the type of sample introduction system used. The sample introduction system is preferably used in an analytical instrument, such as in determining the concentration of an analyte in a sample. A typical introduction system has at least two, but ideally three syringe pumps.

Matrix effects: In ICP-MS, matrix effects represent a critical aspect because the sample matrix can impact the ionization efficiency and the detection of elements. Matrix effects cause errors in quantitation, and thus have to be tightly controlled to get high accuracy in ICP-MS.

Interference correction: In ICP-MS, interference correction is the most important step because interference from other elements affects the accuracy of detection. Advanced interference correction techniques have improved the accuracy of ICP-MS, allowing trace elements to be detected in complex samples.

Instrument calibration: Calibration of the instrument is the important step of ICP-MS, wherein the instrument is calibrated to have the accurate detection of elements. Calibration involves the optimization of parameters of the instrument, such as RF power, gas flow and detector settings.

Quality control: Quality control is the critical aspect of ICP-MS, wherein quality of the data generated is ensured by using quality control samples and protocols. The implementation of quality control measures will be essential toward achieving high accuracy and reliability of ICP-MS. At the end of each quality management section are some of the most salient CAP (College of American Pathologists) regulations as well as useful aids for carrying out active quality control and for surveillance of laboratory performance through quality assurance analyses [17].

3.8 Proximate Analysis:

Proximate analysis is a laboratory technique used to determine the chemical composition of a substance, typically food, feed, or environmental samples. Proximate analysis is often used as a preliminary step in more detailed chemical analysis or to evaluate the quality and properties of a substance. Proximate analysis of sand samples provides information on the physical and chemical composition of sand including moisture content, organic matter, ash content and inorganic constituents like silica, iron, and aluminum. This technique is applied across numerous industries, e.g., construction, mining, and environmental surveying, for assessing the properties and quality of sand, whether it is acceptable for use in construction, filtering, or other purposes. Knowing the proximate composition of sand, manufacturers and scientists can spot potential impurities, maximize the conditions of processing and satisfy regulatory requirements. Proximate analysis is generally carried out by using American Society for Testing and Materials (ASTM) and Indian Standard (IS) methods. This analysis consists of four groups: moisture, ash (The inorganic residue after combustion), volatile matter (Consisting of gases and vapor driven off during pyrolysis) and fixed carbon.

3.9 Sample Preparation for Proximate Analysis (ASTM D7582-15):

For sample preparation, Sand samples were crushed with a mortar and pestle, then further crushed in a Rotor Beater Mill to 212 µm, then sieved in a Sieve Shaker Machine. The produced sample was then utilized for analysis and investigations.

3.9.1 Determination of Moisture Content:

Procedure:

1. Weigh a known amount of air-dried sample (about 1 g).
2. Place in a moisture oven at 105 ± 5°C for at least 1 hour or until constant weight.
3. Cool in a desiccator and weigh.

Calculation:

$$\text{Moisture } (\%) = (W_1 - W_2 / W_1) \times 100$$

Where: W_1 = Weight of sample before drying.

W_2 = Weight after drying.

3.9.2 Determination Volatile Matter Content:

Procedure:

1. Use the moisture-free sample.
2. Place in a covered crucible (with a snug-fitting lid).
3. Heat in a muffle furnace at 950 ± 20°C for 7 ± 0.5 minutes in the absence of air.
4. Cool in a desiccator and weigh.

Calculation:

$$\text{Volatile Matter } (\%) = (W_3 - W_4 / W_3) \times 100$$

Where:

W_3 = Weight of moisture-free sample.

W_4 = Weight after volatilization.

3.9.3 Determination of Ash Content:

Procedure:

1. Use the residue from volatile matter or a new moisture-free sample.
2. Heat in an open crucible at 750 ± 50°C for at least 1 hour until complete combustion (constant weight).
3. Cool in a desiccator and weigh.

Calculation:

$$\text{Ash (\%)} = (W_5 / W_3) \times 100$$

Where:

W_5 = Weight of ash after combustion

W_3 = Weight of original moisture-free sample

3.9.4 Determination of Fixed Carbon:

The fixed carbon content of sand is essentially negligible, as sand is an inorganic, non-living substance composed of mineral particles. Fixed carbon content typically refers to the amount of carbon remaining in a substance after volatile matter has been driven off, usually measured in the context of biomass or coal.

Calculation:

Fixed carbon content (%) = 100 – {moisture (%) + ash (%) + volatile matter (%)}

Result and Discussion:

The inductively coupled plasma-mass spectroscopy (ICP-MS) technique was used for elemental studies on 18 samples of sand. All the calibration graphs are linear within the stated range for each element. For most of the items in this study, the square of the correlation. Falls between 0.9985 and 0.099999. Good values of precision were obtained. Results are presented in the following figure:

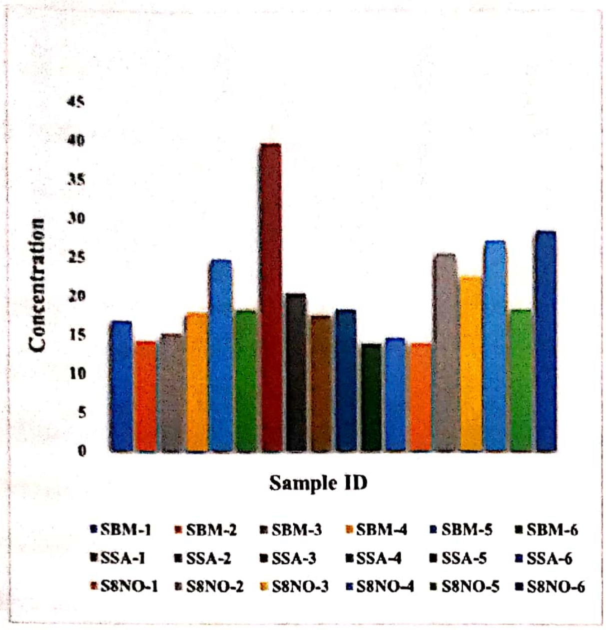

Fig 13: Distribution plot for Li (ppm) in sand

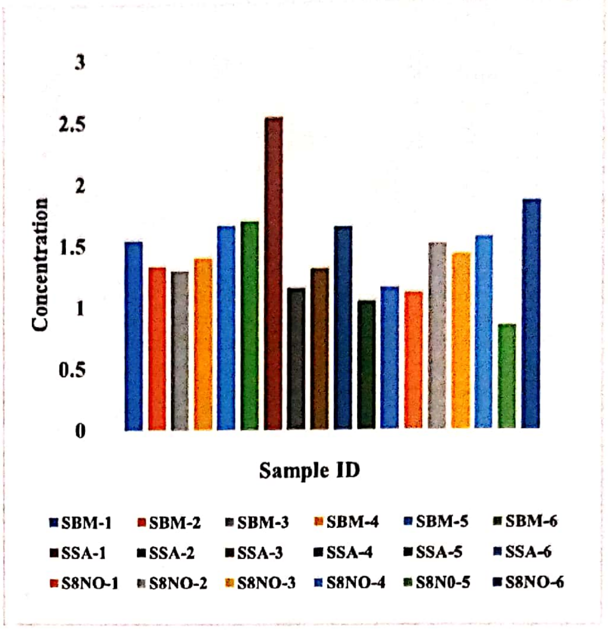

Fig 14: Distribution plot for Be (ppm) in sand

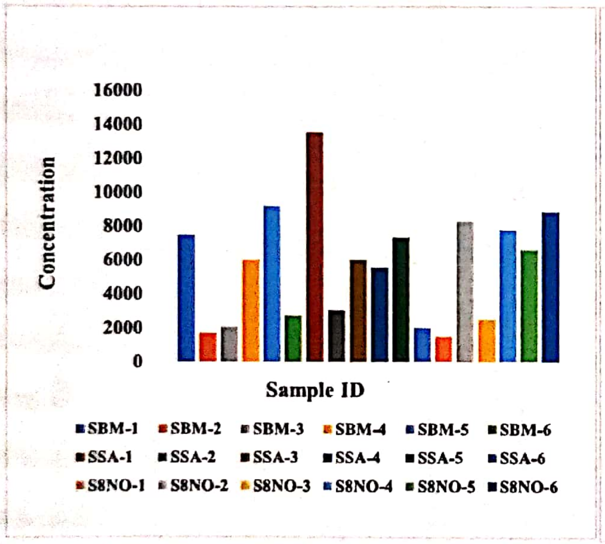

Fig 15: Distribution plot for Mg (ppm) in sand

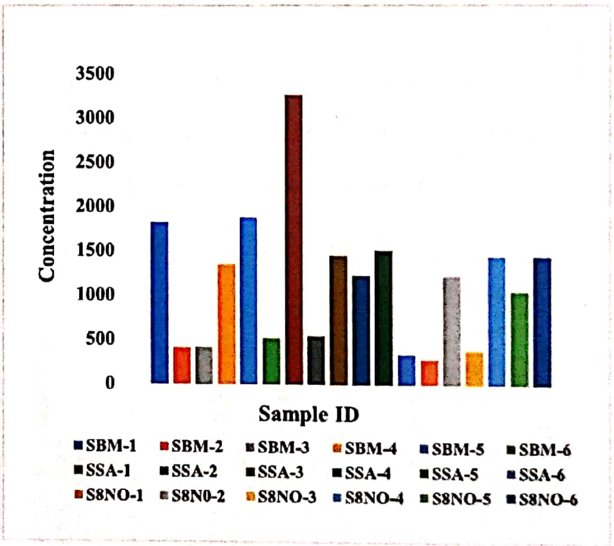

Fig 16: Distribution plot for Ca (ppm) in sand

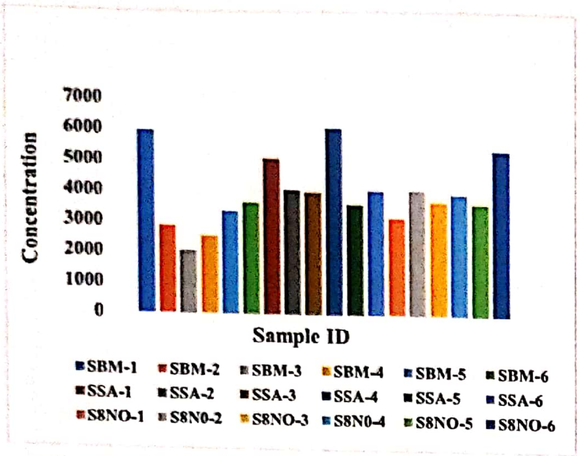

Fig 17: Distribution plot for Ti (ppm) in sand

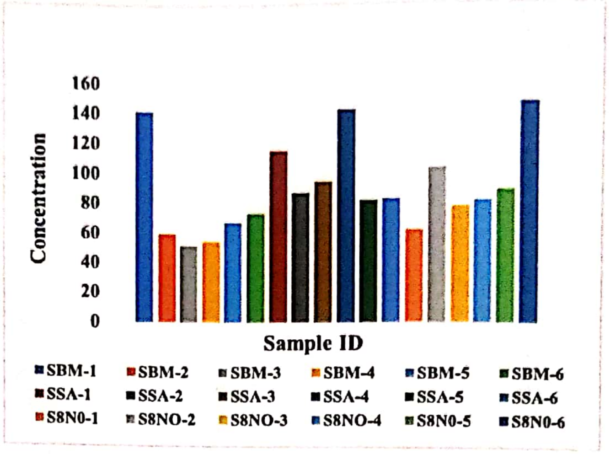

Fig 18: Distribution plot for V (ppm) in sand

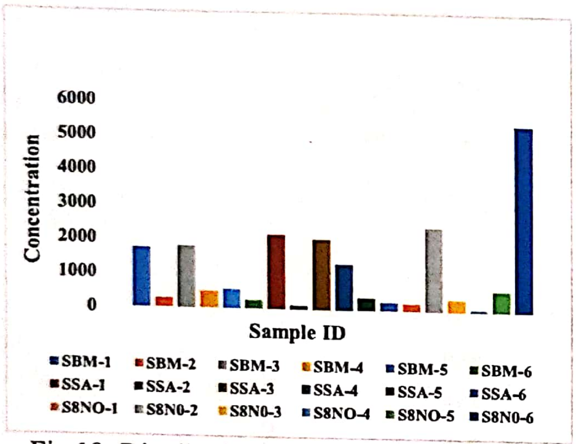

Fig 19: Distribution plot for Cr (ppm) in sand

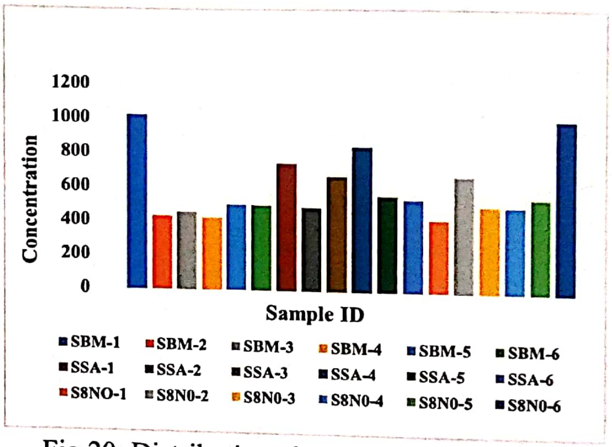

Fig 20: Distribution plot for Mn (ppm) in sand

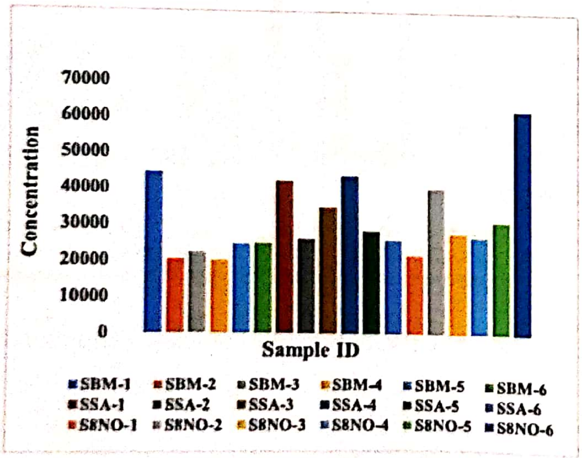

Fig 21: Distribution plot for Fe (ppm) in sand

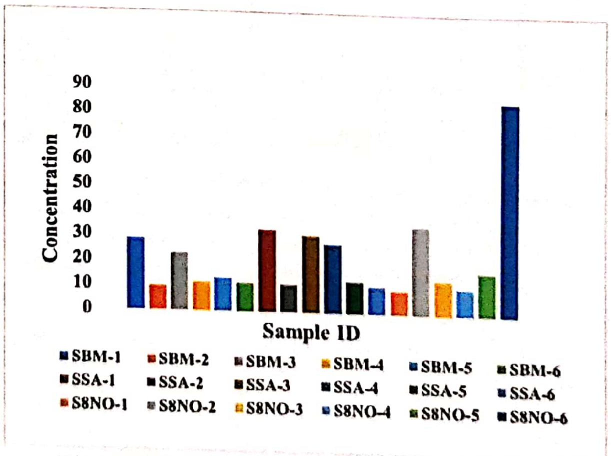

Fig 22: Distribution plot for Co (ppm) in sand

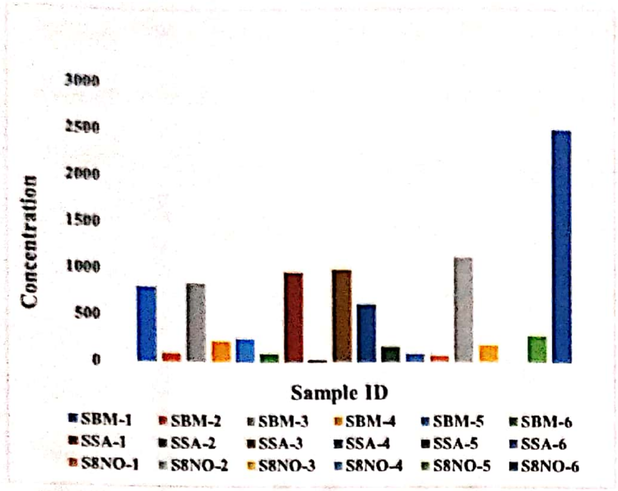

Fig 23: Distribution plot for Ni (ppm) in sand

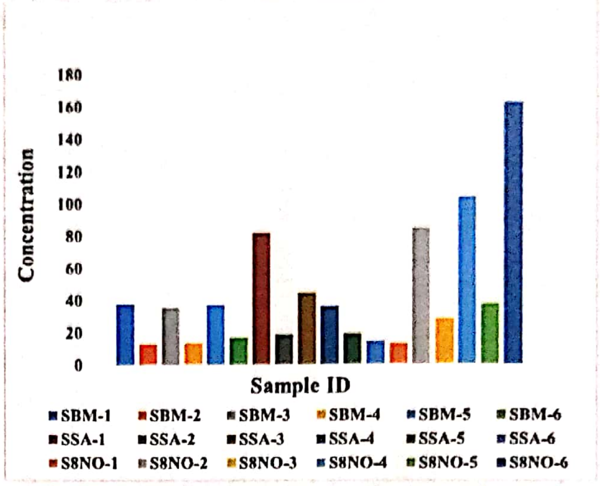

Fig 24: Distribution plot for Cu (ppm) in sand

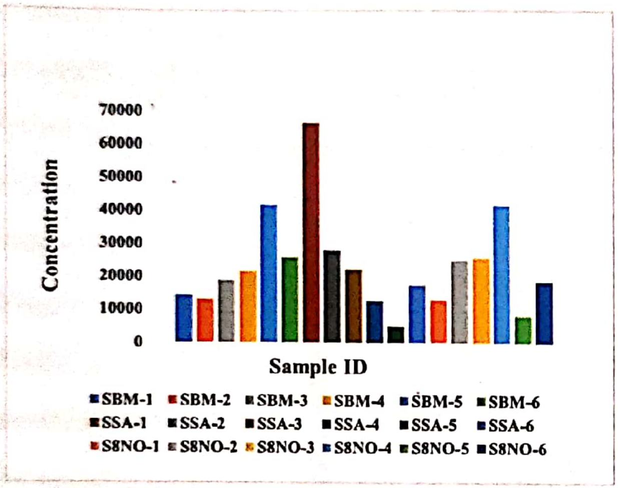

Fig 25: Distribution plot for Zn (ppm) in sand

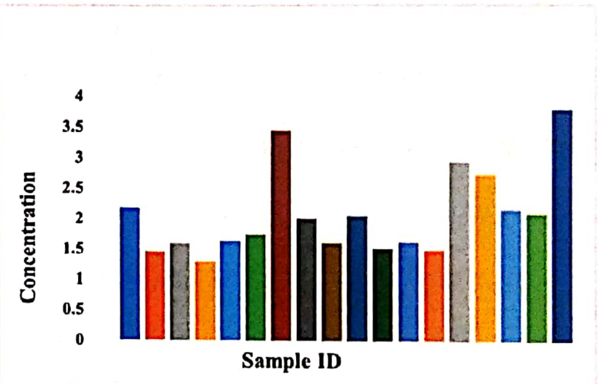

Fig 26: Distribution plot for As (ppm) in sand

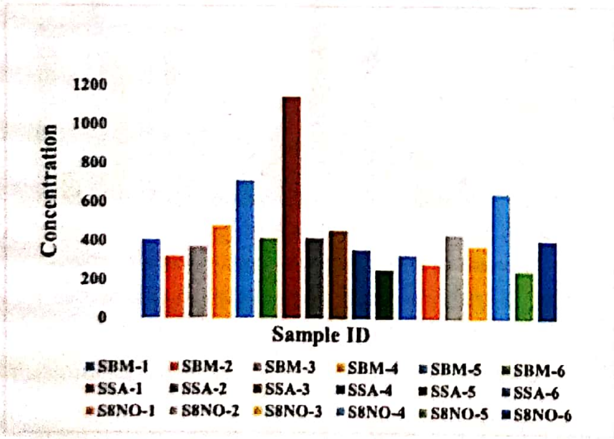

Fig 27: Distribution plot for Sr (ppm) in sand

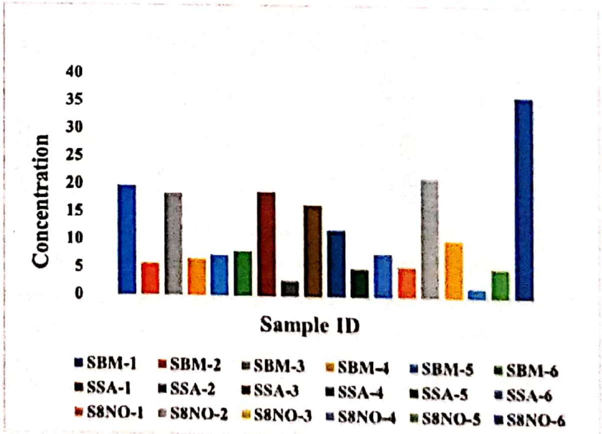

Fig 28: Distribution plot for Mo (ppm) in sand

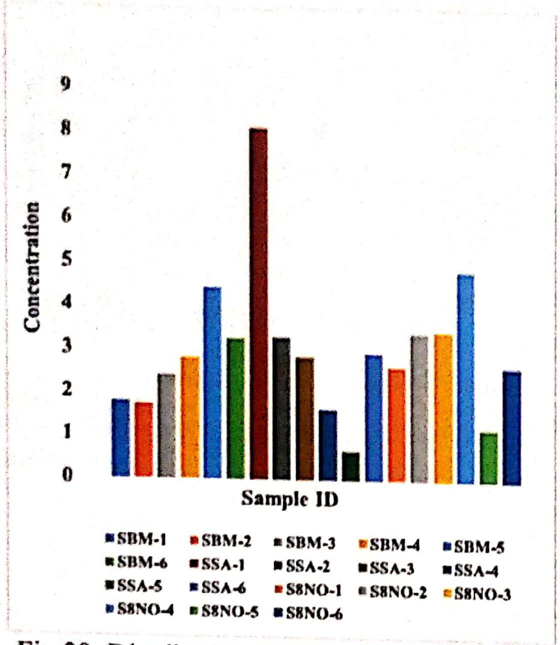

Fig 29: Distribution plot for Cd (ppm) in sand

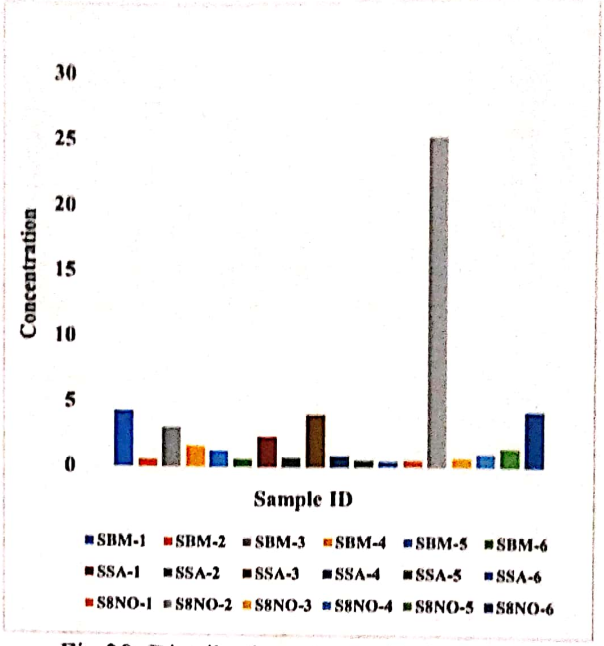

Fig 30: Distribution plot for Sb (ppm) in sand

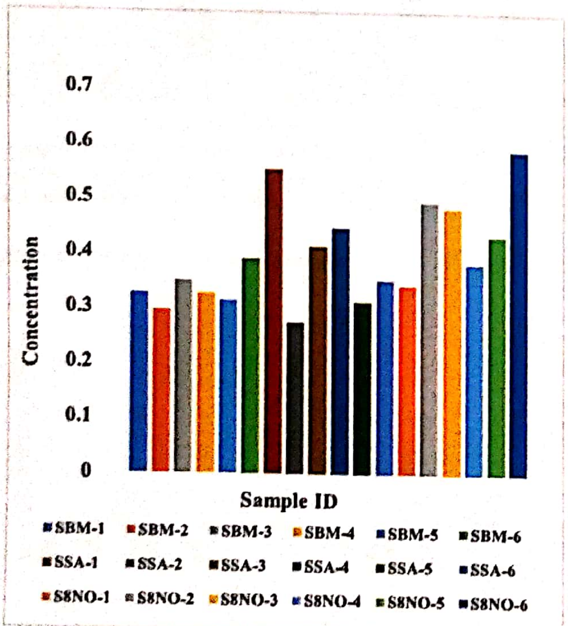

Fig 31: Distribution plot for Tl (ppm) in sand

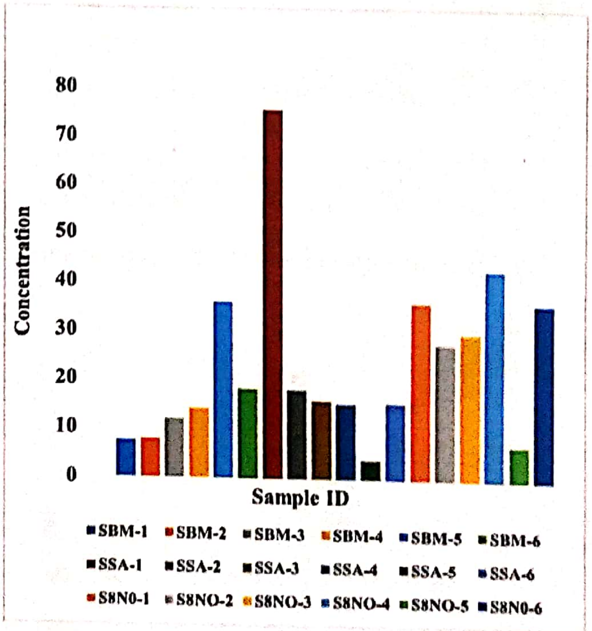

Fig 32: Distribution plot for Pb (ppm) in sand

The following tables and figures detail the concentrations of a very wide variety of elements, including lithium (Li), beryllium (Be), magnesium (Mg), calcium (Ca), titanium (Ti), vanadium (V), chromium (Cr), manganese (Mn), iron (Fe), cobalt (Co), nickel (Ni), copper (Cu), zinc (Zn), arsenic (As), strontium (Sr), molybdenum (Mo), cadmium (Cd), antimony (Sb), thallium (Tl), and lead (Pb), which have been detected in multiple samples collected with extreme care from three different geographical locations: Shanti Ashram, abbreviated as SSA, 8No. Spur and labeled as S8NO and Baghmora, labeled as SBM. The samples from Shanti Ashram (SSA) have shown to contain highly Fe content, and particularly high values were seen in sample SSA-2, which registered a very high value of 45,796.16 ppm, and Zn was found in considerable amount in sample SSA-4 at 50,543.4 ppm. Though Cr levels in these samples are moderate, yet in sample SSA-3, it has shown a significant concentration of 1,455.606 ppm. The samples taken from the 8NO Spur site show the highest concentrations of Fe, especially at an outstanding 62,471.58 ppm in both samples S8NO-4 and S8NO-5, with significant Cr concentrations at 7,285.167 ppm in sample S8NO-4. Zn and Sr also have notable concentrations in these samples, with Zn reaching an impressive 41,835.44 ppm in sample S8NO-2. In addition, trace elements Sb, Cd, and Tl have been found uniformly distributed in all the sampled sites, but with minor concentration increases at some samples taken from the S8NO site. Fe and Zn are the elements that dominate the samples analyzed with the highest values recorded in samples S8NO-4 and S8NO-5 while Cr is higher in both samples, S8NO and SSA. In the samples collected from Baghmora, it was established that Fe and Cr were highly concentrated, with Fe showing an excellent peak concentration of 44,383.92 parts per million (ppm) in sample SBM-1, and Cr showed an apex concentration of 2,735.192 ppm in sample SBM-2. Other elements of notable interest include Mn, Zn and Sr; it is worthwhile mentioning the enhanced values for Zn recorded at 25,825.41 ppm, while Sr values amount to

810.02 ppm in sample SBM-6. This detailed study helps to elucidate the geochemical diversity as well as the spatial distribution of the elements contained within the samples of sand that were collected in a variety of contextual environments.

Lithium (Li): The presence of Li in river sand mainly depends on the natural weathering and erosion of rocks containing lithium-bearing minerals; among the best examples are spodumene or lepidolite. These minerals get broken down with the mechanical processes resulting from water flow, which carries tiny particles of Li into riverbeds. With water and time, it carries materials from the surrounding geological formations thus depositing some material to be eroded and stacked up in riverbank sands, silts, and gravels. There exists besides natural weathering also leaching out of minerals from surrounding rocks, leaving trace amounts of Li in the river sands. This process is part of the natural cycle whereby elements' parts are redistributed from one region across the landscape sometimes concentrating valuable minerals like Li.

Beryllium (Be): Be is in river sand, mainly as a result of the weathering and erosion of beryl-rich or bertrandite-containing rocks. When such rocks get decomposed, they release Be from the earth environment. Water carrying the particles containing beryllium-rich minerals from the rock formations at an upstream position dumps them at specific points in a river bed and settles as river sand. Be is usually present in trace amounts in these sediments, as it is a relatively rare element. The process of leaching, where water dissolves minerals from rocks, also plays a role in the distribution of Be in river sands, gradually moving it from the parent rock into the sedimentary environment.

Magnesium (Mg): River sands contain most of their Mg from weathering and erosion of magnesium-rich minerals such as olivine, serpentine, or dolomite, present in rocks of many kinds, including igneous and sedimentary. As years go by, these rocks are fragmented due to processes like rainfall, river flow, and temperature variations, releasing Mg ions into the surroundings. As water flows through these rocks and sediments, it carries Mg in both dissolved form and as part of mineral particles. The Mg then accumulates in the river sand and sediment as the water transports it downstream. Moreover, chemical weathering, which is the reaction of minerals with water and atmospheric gases, contributes to the release of Mg, which becomes part of the river's sedimentary load.

Calcium (Ca): The presence of Ca in river sands is mainly related to the decomposition and erosion of highly calcium-rich minerals, such as calcite and gypsum and dolomites, which compose sedimentary limestone. These decompose over thousands of years through normal weathering-both mechanical damage by flowing waters and chemical change due to action with rainwaters or atmospheric CO_2. As these rocks erode, Ca in the form of ions or small mineral particles is carried by the river's flow and deposited in the sand and sediment along the riverbed. In addition to direct mineral weathering, Ca can also be released into the river system through the dissolution of calcium carbonate ($CaCO_3$), which is common in areas with limestone or chalk deposits. As a consequence, Ca is often accumulated in river sands as part of the overall sedimentary load.

Titanium (Ti): The presence of Ti in river sand is mainly because of the erosion and weathering of titanium-containing minerals such as ilmenite and rutile, which are present in igneous and metamorphic rocks. These minerals are resistant to chemical weathering, so they remain relatively stable even as other rocks break down over time. As natural forces, such as wind, water, and temperature changes weather the rocks with these minerals, titanium-bearing particles find their way to the environment. River water is responsible for the transportation of such particles, leading to accumulation within river sand and sediment, primarily in areas whose bedrock holds titanium-bearing minerals. Rivers sands can also be concentrated with Ti through practices such as heavy mineral separation, where denser minerals such as ilmenite settle from the water and become concentrated in specific areas, increasing the intensity of Ti in such sands.

Vanadium (V): The presence of V in river sand is primarily due to the weathering and erosion of rocks that contain vanadium-bearing minerals, such as vanadinite, patronite, or vanadiferous shale. Over time, these parent rocks break down due to natural processes like physical erosion and chemical weathering. During this process, V is released into the surrounding environment in the form of dissolved ions or mineral particles. As rivers carry these weathered materials from upstream regions, V can be concentrated in river sand and sediments. Moreover, V may be concentrated in specific areas of river sand by processes such as sorting by particle size or density, since heavier minerals tend to settle out of the water and become more concentrated. Although V is present in trace amounts in river sand, it may be an important element in areas where vanadium-bearing rocks are concentrated.

Chromium (Cr): Chromium (Cr) is often assumed to have natural and anthropogenic sources in river sand. Natural sources include the weathering and erosion of chromium-rich rocks, including ultramafic and serpentinized rocks, that release the element into surrounding soils and water systems. The geological composition of the catchment area determines the amount of Cr present in the sand. Other major sources of Cr contamination are industrial effluents from leather tanning, electroplating, mining, and metallurgical activities. In areas where untreated industrial discharge or improper waste management is prevailing, Cr content in river sediments is generally found to be higher. Also, agricultural runoff containing Cr-based pesticides and fertilizers may also enhance its availability. The mobility and deposition of Cr in river sand depend on its hydrodynamics, pH, and redox condition, which generally influence its transportation and accumulation.

Manganese (Mn): The influx of Mn into river sand is mainly determined by both natural geological processes and human action. Naturally, some river systems receive Mn through the weathering of Mn-rich minerals and rocks, including pyrolusite and rhodochrosite, in the catchment area surrounding the river. Weathering mechanisms are further influenced physically, chemically, and biologically, causing this Mn to be washed into river sediments. Anthropogenic activities, such as mining, industrial discharge, and urban runoff, may elevate levels of Mn in river sand. Herein, wastewater from metallurgical industries, steel production, and fertilizer application often contains relatively high concentrations of Mn. Moreover, agricultural uses of manganese-based fertilizers and pesticides result in leaching, thus being carried away into rivers. The deposition of Mn in river sand is influenced by sedimentation rates, water flow, and the environmental conditions that prevail in an area, like pH and redox potential that influence the solubility of Mn; hence, its final deposits in sediments.

Iron (Fe): The presence of iron (Fe) in river sand is essentially a result of natural geological processes and, to a lesser extent, human activities. Fe is abundant in the Earth's crust and is naturally released into river systems through the weathering and erosion of Fe-rich rocks and minerals, including hematite, magnetite, and siderite. These processes are driven by physical forces such as water flow and chemical reactions; the two groups of chemical reactions include oxidation and hydrolysis. Other sources of iron include volcanic activities and transported iron-bearing sediments sourced from upstream regions. Other man-made sources of iron contamination in river sand are from mining, industrial effluent, and urban runoff. Smelting, ore processing industries, and manufacturing firms often leave small or large amounts of waste products containing iron into the connected water bodies. Hydrodynamic conditions, redox states, and pH levels affect the solubility and precipitation of iron into sediments and control its deposition and concentration in river sand.

Cobalt (Co): River sand in most instances contains Co, which mainly originates from weathering and erosion of cobalt-rich rocks and minerals upstream. When water is allowed to move along the geology containing ores like laterites, ultramafic rocks, and particular sulphide deposits, it transfers cobalt particulates downstream slowly. Industrialization, mining, and atmospheric depositions can be contributing factors of Co pollution in river sands. Over time, these natural and anthropogenic processes result in the cobalt accumulating in river sediments.

Nickel (Ni): Presence of Ni in sand is due to weathering and erosion of nickel-rich rocks like ultramafic and lateritic formations. They release nickel in the river system. Human activity contributes to it also, as seen in the forms of mining, industrial discharge, and atmospheric deposition from the operation of smelting plants. All these natural and anthropogenic sources influence the Ni content in river sand.

Copper (Cu): The presence of copper (Cu) in river sand is primarily through the weathering and erosion of copper-bearing rocks and minerals, such as chalcopyrite, malachite, and bornite, which release Cu particles into the river system. Natural processes, such as leaching from soil and volcanic activity, also introduce it. Moreover, human activities, including mining, industrial discharge, and agricultural runoff, may introduce Cu into river sediments. These combined natural and anthropogenic sources affect the concentration of copper in river sand.

Zinc (Zn): The main reasons for the presence of zinc (Zn) in river sand are due to the weathering and erosion of zinc-bearing minerals, such as sphalerite and smithsonite, from surrounding rock formations. Other natural processes such as leaching, volcanic eruptions, and hydrothermal alterations will contribute to its release into the river system. Human activities like mining, disposal of industrial wastes, and agricultural runoff also introduce Zn into river sediments. These combined natural and anthropogenic factors determine the Zn content in river sand.

Arsenic (As): Main sources of arsenic (As) in river sand are the weathering and erosion of arsenic-bearing minerals present in surrounding rocks including arsenopyrite, realgar, and orpiment. Other natural sources include geothermal activity, volcanic emissions and leaching from soils. Anthropic sources include mining, industrial discharge, pesticide use, and improper disposal of wastes that may introduce the metalloid to river sediments. These combined natural and human-induced factors influence arsenic concentration in river sand.

Strontium (Sr): Strontium (Sr) is mostly present in river sand as a result of weathering and erosion of strontium-bearing minerals, including celestine ($SrSO_4$) and strontianite ($SrCO_3$), from surrounding rock formations. Its presence also comes from natural leaching from carbonate rocks, marine sediments, and volcanic activities. Other than these natural factors, industrial discharge, agricultural runoff, and mining can also add Sr to river sediments. Natural and anthropogenic factors are considered to be a combination of influencing Sr content in river sand.

Molybdenum (Mo): The primary reason for the occurrence of molybdenum (Mo) in river sand is the weathering and erosion of molybdenum-bearing minerals such as molybdenite (MoS_2) from the surrounding rock formations. Volcanic activities, hydrothermal alterations, and leaching from soil are natural processes that lead to its occurrence. Mo can also enter river sediments through anthropogenic sources such as mining, industrial discharge, and agricultural runoff. These combined natural and human-induced factors influence the concentration of Mo in river sand.

Cadmium (Cd): The reason for the abundance of cadmium (Cd) in river sand is through weathering and erosion of minerals carrying Cd like greenockite (CdS), often bound with zinc minerals, particularly with sphalerite. Cd also finds entry through natural leaching from the rocks, volcanic activities, and hydrothermal alteration. Besides that, it finds its entry due to various industrial sources, namely mining, effluent release, battery disposal, and agricultural run-off originating from phosphate fertilizers. These combined natural and human-induced factors influence the Cd concentration in river sand.

Antimony (Sb): The main source of Sb in river sand is due to the weathering and erosion of antimony-bearing minerals such as stibnite (Sb_2S_3) from the surrounding rock formations. It also comes through natural processes, such as volcanic activity, geothermal emissions, and leaching from soils. Besides these factors, human activities such as mining, industrial discharge, smelting operations, and waste runoff also introduce Sb into river sediments. Together, these factors control the Sb concentration in river sand.

Thallium (Tl): Thallium (Tl) mainly occurs in river sand as a result of weathering and erosion of thallium-bearing minerals, including lorandite and crookesite, commonly associated with the sulfide ores of lead, zinc, and copper. Its presence also occurs from natural sources, including volcanic activity, hydrothermal processes, and leaching from rocks. Tl also finds its way into river sediments through various human activities like mining, industrial waste discharge, and smelting operations. Thus, these factors, both natural and human-induced, control the concentration of Tl in river sand.

Lead (Pb): The lead (Pb) presence in river sand primarily arises from the weathering and erosion of lead-bearing minerals, mostly galena (PbS), from the surrounding rock formations. Natural sources include leaching from soil, volcanic action, and hydrothermal alteration. Anthropogenic sources include mining, industrial discharge, lead-based paints, and contamination from leaded gasoline in the past that actually introduced Pb into river sediments.

Table 5: Proximate analysis results of sand samples.

Samples	**Moisture Content**	**Volatile Matter**	**Ash Content**	**Fixed Carbon**	**Method**
SBM-1	0.31	0.5	99.19	0	ASTM D7582-15
SBM-2	0.33	0.4	99.27	0	
SBM-3	0.23	0.4	99.37	0	
SBM-4	0.24	0.02	99.74	0	
SBM-5	0.36	0.2	99.44	0	
SBM-6	0.47	0.11	99.42	0	
SSA-1	0.72	1.5	97.78	0	
SSA-2	0.53	1.02	98.45	0	
SSA-3	0.54	1.01	98.45	0	
SSA-4	1.02	1.05	97.93	0	
SSA-5	0.31	0.4	99.29	0	
SSA-6	0.38	0.6	99.02	0	
S8NO-1	0.41	0.9	98.69	0	

Proximate analysis of sand samples indicates a variety of physical and chemical properties. Moisture content ranges from 0.23% (SBM-3) to 1.02% (SSA-4), with SSA samples showing higher moisture than SBM samples. Volatile matter is maximum in SSA-1 at 1.5%, followed by SSA-4 (1.05%) and SSA-2 (1.02%), and minimum in SBM-4 (0.02%). Ash content is always high in all samples, reflecting the dominance of inorganic material, ranging from 97.78% (SSA-1) to 99.74% (SBM-4). SBM samples show greater ash content and less moisture and volatile matter, while SSA samples show relatively lower ash and greater organic-related contents. All samples showed 0% fixed carbon, ascertaining the insignificant presence of residues based on carbon. These findings indicate both spatial and compositional variation in the sediment profile along the Brahmaputra River shoreline.

5. Conclusion:

The study reveals that the river sand exhibits a complex and varied chemical composition. The concentration of heavy metals varied spatially in the river sand, influenced by factors like the source rock composition, weathering intensity, and transport distance. The research methodology involved a detailed procedure. This included meticulously collecting river sand samples from three locations - Shanti Ashram, 8 No Spur, and Baghmora. The samples were air-dried, crushed using a Rotor Beater Mill, and sieved before being digested in a microwave-assisted digestion process. The digested samples were then diluted and analyzed using ICP-MS. The study found significant concentrations of Fe, Cr, and Zn in the river sand, with varying concentrations observed across the three locations. The samples from Shanti Ashram (SSA) have shown to contain highly Fe content, and particularly high values were seen in sample SSA-2, which registered a very high value of 45,796.16 ppm, and Zn was found in considerable amount in sample SSA-4 at 50,543.4 ppm. The highest concentrations of Fe were found at the 8No Spur site, with samples S8NO-4 and S8NO-5 showing significant concentrations (62,471.58 ppm). The Baghmora samples showed an excellent peak concentration of Fe (44,383.92 ppm in SBM-1) and Zn (25,825.41 ppm in SBM-6). The findings highlight the importance of understanding the factors controlling the distribution of heavy metals in river sand, as it has implications for various applications. It also emphasizes the need for further research to assess the potential environmental risks associated with heavy metal contamination in river sand.

Proximate analysis of shoreline sand samples from the Brahmaputra River at Jorhat, Assam, exhibits significant spatial and compositional heterogeneity. The moisture content varied from 0.23% in SBM-3 to 1.02% in SSA-4, with SSA samples having higher moisture content in general. Volatile matter was maximum in SSA-1 (1.5%) and minimum in SBM-4 (0.02%), reflecting a greater organic content in the SSA area. Ash content remained highest in all the samples, varying from 97.78% in SSA-1 to 99.74% in SBM-4, indicating the prevalence of inorganic mineral matter, especially in SBM samples. All the samples had 0% fixed carbon, ascertaining negligible existence of residues based on carbon. It is indicated that SSA sites have relatively higher organic-rich sediments and SBM sites consist mainly of mineral material. The disparity in these parameters indicates differences in depositional settings and sediment sources along the river, highlighting the necessity for continued geochemical monitoring and environmental management in the area.

6. Reference

1. The Civil Engineering. (2024, August 8). What is sand? | 27 types of sand (classification of sand). Retrieved from https://thecivilengineering.com/what-is-sand/
2. Cement Concrete. Types of sand: Uses, properties, grain size & classification. Retrieved from https://cementconcrete.org/construction-materials/types-of-sand-grain-size/2667/
3. Tanaka, K., & Watanabe, N. (2015). Size distribution of alkali elements in riverbed sediment and its relevance to fractionation of alkali elements during chemical weathering. Chemical Geology, 411, 12–18.
4. Habersack, H., & Kreisler, A. (2012). Dating torrential processes on fans and cones. In Sediment transport processes (pp. 51–73). Springer.
5. Chandrasekaran, A., Senthil Kumar, C. K., Sathish, V., Manigandan, S., & Tamilarasi, A. (2021). Effect of minerals and heavy metals in sand samples of Ponnai River, Tamil Nadu, India. Scientific Reports, 11, Article 23199. https://doi.org/10.1038/s41598-021-02596-5
6. Debnath, A., Singh, P. K., & Sharma, Y. C. (2024). Spatial distribution of heavy metals in the sediments of River Ganges, India: Occurrence, contamination, source identification, seasonal variations, mapping, and ecological risk evaluation. Marine Pollution Bulletin, 198, 115910. https://doi.org/10.1016/j.marpolbul.2023.115910
7. Gupta, D., Shukla, R., Srivastava, P. K., & Mishra, V. K. (2024). Assessment of heavy metal pollution level, ecological and human health risks in surface water of Narmada River, India. Sustainable Water Resources Management, 10(1), Article 154. https://doi.org/10.1007/s40899-024-01131-1
8. Rana, M. S., Shahriar, M. S., Alam, M. S., Hossain, M. I. S., Biswas, P., & Zaman, M. N. (2023). Evaluation of foundry properties of Brahmaputra River sand and its prospects. Archives of Foundry Engineering, 2023(2), 80–90. https://doi.org/10.24425/afe.2023.144299
9. Chakarvorty, M., Dwivedi, A. K., Shukla, A. D., Kumar, S., Niyogi, A., Usmani, M., Pati, J. K. (2015). Geochemistry and magnetic measurements of suspended sediment in urban sewage water vis-à-vis quantification of heavy metal pollution in Ganga and Yamuna Rivers, India. Environmental Monitoring and Assessment, 187(9). https://doi.org/10.1007/s10661-015-4794-x
10. Falciani, R., Novaro, E., Marchesini, M., & Gucciardi, M. (2000). Multi-element analysis of soil and sediment by ICP-MS after a microwave-assisted digestion method. Interlaboratory Note. Published on the Web April 25, 2000.
11. Suleman, N. M., & ElAgib, I. (2015). Quantitative and qualitative analysis of sand in Nafud Desert at Zilfi Province using (ICP-MS) spectroscopic technique. Journal of Engineering and Applied Sciences, 2(1), 17–26.
12. Veerasamy, N., Sahoo, S. K., Murugan, R., Kasar, S., Inoue, K., Fukushi, M., & Natarajan, T. (2021). ICP-MS measurement of trace and rare earth elements in beach placer-deposit soils of Odisha, East Coast of India, to estimate natural enhancement of elements in the environment. Molecules, 26(24), 7510. https://doi.org/10.3390/molecules2624751
13. Aggarwal, M., Anbukumar, S., & Kumar, T. V. (2024). Measurement of heavy metals content in suspended sediment of Ganges River using atomic absorption spectrometry. MAPAN, 39, 913–930.
14. Brcka, J. (2003). Integrated electrostatic inductive coupling for plasma processing. Tokyo Electron.

15. Jeon, S. J., Tolmachev, Y. N., Lee, S. H., Seok, S. H., Park, Y. M., & Jang, W. H. (2008). Plasma generating apparatus. Samsung.
16. Barnett, E. F., Tandler, W. S. W., & Turner, W. R. (1968). Quadrupole mass filter with fringing-field penetrating structure. U.S. Patent No. 3,389,323.
17. Bormann, C. L., & Racowsky, C. (2012). Ongoing quality assessment/improvement in clinical IVF. In In vitro fertilization: A comprehensive guide (pp. 225-247). Springer.

7. Photo Gallery

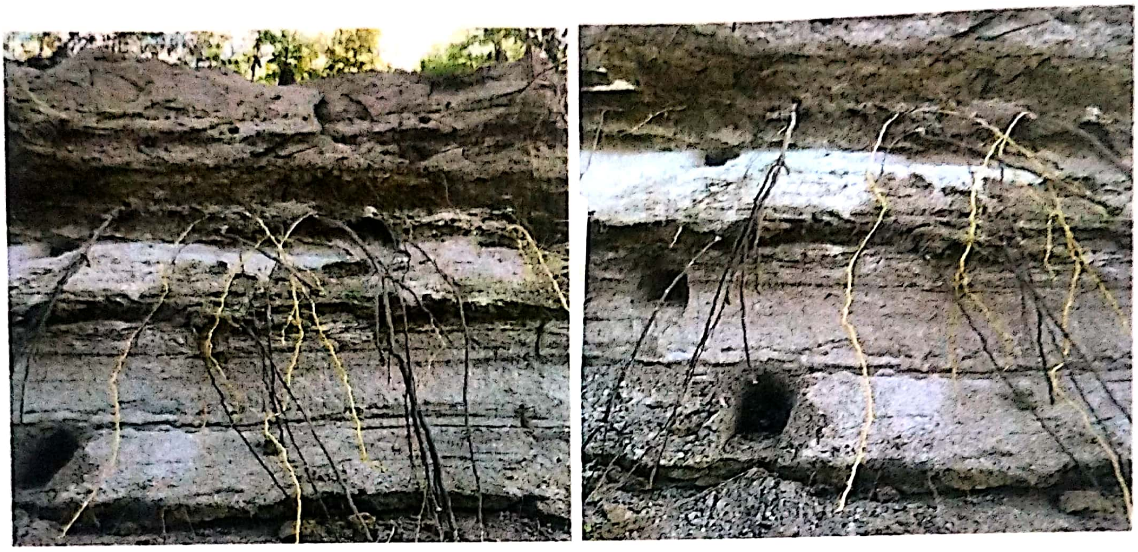

Fig 1: Sample Collection from different depth of shoreline of the Brahmaputra.

Fig 2: Air dry process.

Fig 3: Samples after oven dry.

Fig 4: Rotor Beater Mil (4000 RPM)

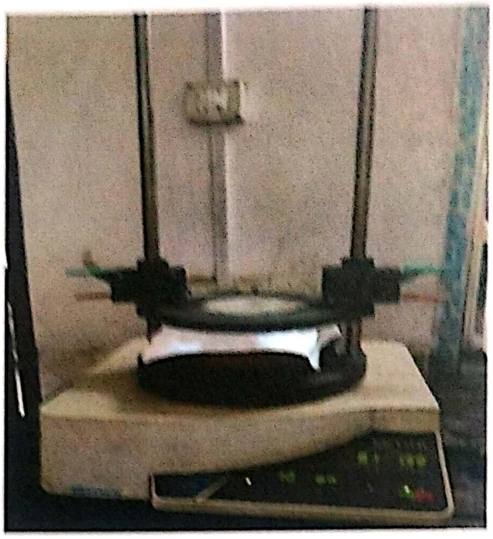

Fig 5: Sieve Shaker Machine (72 BS)

Fig 6: Analytical Balance

Fig 7: Hot air oven

Fig 8: During sample dilution process

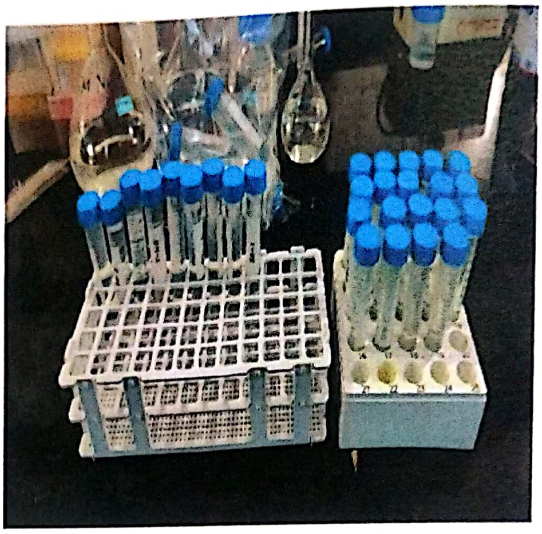

Fig 9: Centrifuge Tube

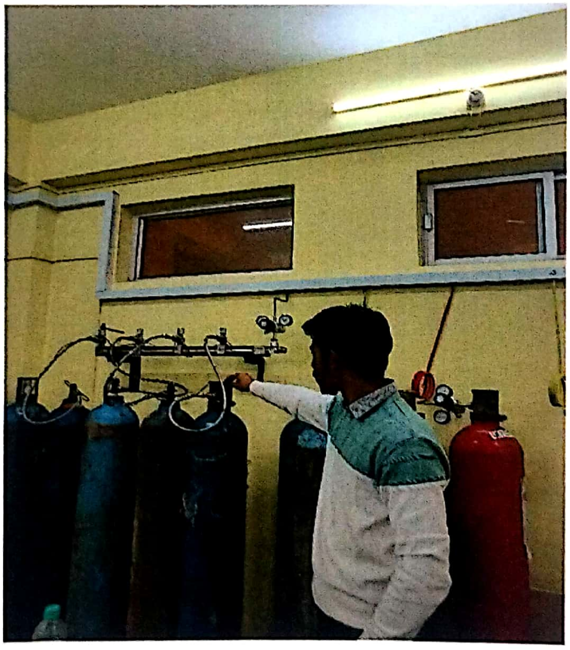

Fig 10: Argon gas cylinder